Rich-Media Tags: Battery-Free Wireless Multichannel Digital Audio and Image Transmission with UHF RFID Techniques

Stewart J. Thomas*, Travis Deyle*, Reid Harrison† and Matthew S. Reynolds*
*Department of Electrical and Computer Engineering, Duke University, Durham, NC
†Intan Technologies LLC, Los Angeles, CA

***Abstract*—In this paper we present the first fully passive (battery-free) wireless transmission of multiple digital audio channels and images via modulated backscatter. We leverage a previously reported single chip, passive transponder that can digitize and uplink up to 10 analog input channels sampled at a rate of 26.1 kHz. Given a base station transceiver operating at a frequency of 915 MHz and a transmit power of +36 dBm EIRP, the transponder has a demonstrated operating range of ≈1.4 m. The transponder data uplink uses binary phase-shift key (BPSK) modulated backscatter operating at a total link throughput rate of 5 Mbps, with an uplink energy consumption of only 3.7 pJ/bit.**

The transponder was initially designed for biomedical telemetry of neural and EMG signals. We present a new application of this tag for multichannel, high fidelity digital audio recording, as well as color image transfer using a slow-scan television (SSTV) modulation (*PD290*) with a resolution of 640 by 493 pixels. Additionally, we demonstrate fully-passive digital recording of ambient sound using a microphone powered by the chip's harvested energy at an operating range of 0.72 m. The passive, digital microphone is sensitive enough to record human speech within approximately 5 m of the device. We believe these results will serve as a first step toward media-rich battery-free (wirelessly powered) devices that take advantage of the high speed, low power nature of modulated backscatter communication links.

I. Introduction

Many of the earliest experiments with modulated backscatter communication have involved the transmission of audio signals. For example, in 1880 Alexander Graham Bell presented the *photophone* – a passive device for wireless audio communication [1]. The photophone communicated speech by focusing ambient light onto a mirrored reflecting surface. Sound waves caused the mirror to vibrate and thereby modulated the reflected beam of light. The photophone's receiver used a photo-resistive material to demodulate the incident modulated light beam, and to drive a time-varying current into an earphone to reproduce the original audio signal.

The principle of modulated backscatter was then further developed at radio frequencies, replacing Bell's ambient light source with an RF transmitter collocated with the backscatter receiver. A photophone-like device operating in the UHF frequency range was developed by Leon Theremin in the form of the "The Great Seal Bug" [2]. In what is perhaps the first fully-passive long-range audio backscatter system, the Great Seal Bug telemetered speech by allowing sound waves to deform a thin wall of a cavity resonator connected to a monopole whip antenna. Although the exact timing of Theremin's invention is unclear in the literature, at around the same time Stockman presented backscatter audio transfer at microwave frequencies using a modulated corner reflector as the backscatter modulator [3].

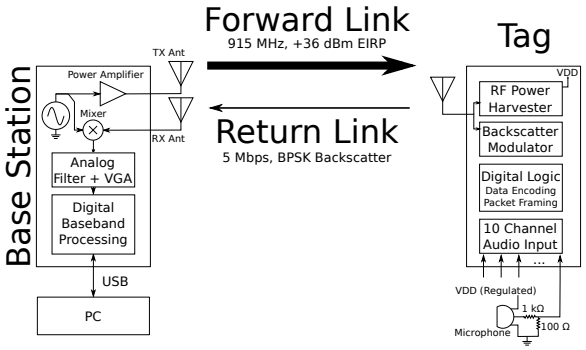

Fig. 1. System block diagram of wireless audio transponder.

The work of these early radio pioneers paved the way for today's RFID and backscatter-based communication systems. Traditional RFID systems, dating as far back as the 1970's, have focused on transmission of short codes for identification and very low-bandwidth, low-resolution sampled sensor data such as temperature information [4]–[8]. Most existing UHF RFID systems communicate using binary ASK or PSK backscatter modulation with data rates from 40-640 kbps. For example, the widely deployed EPC Class 1 Generation 2 RFID protocol is designed for the transmission of short unique-ID and data blocks (eg. 96 bit unique IDs) using a randomized algorithm that results in nondeterminstic throughput [9], [10].

These design decisions in past RFID systems have led to a widely held assumption that modulated backscatter systems are limited to RFID applications and that backscatter is not suitable for streaming transmission of high-bandwidth signals such as high-fidelity digital audio. Recent work has challenged this assumption by demonstrating data rates up to 96 Mbps using 16-QAM backscatter modulation [11], [12].

In this paper, we demonstrate that high bandwidth backscatter links (5 Mbps in this example) can support high fidelity digital audio streaming and image transfer. We present what we believe to be the first fully-passive wireless multichannel high-fidelity digital audio streaming system, as well as the first full color image transmission using a single chip transponder.

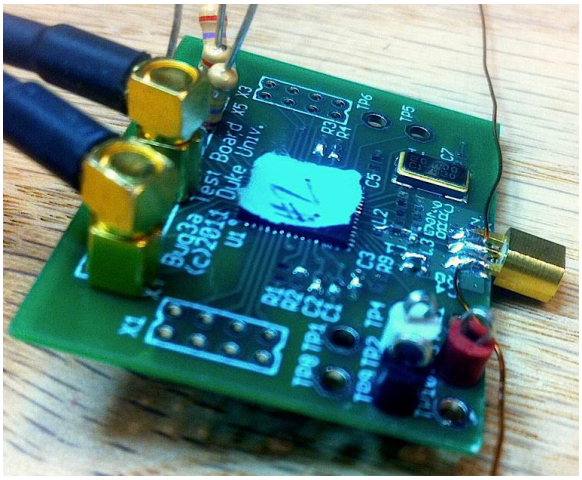

Fig. 2. Photograph of the wireless audio transponder.

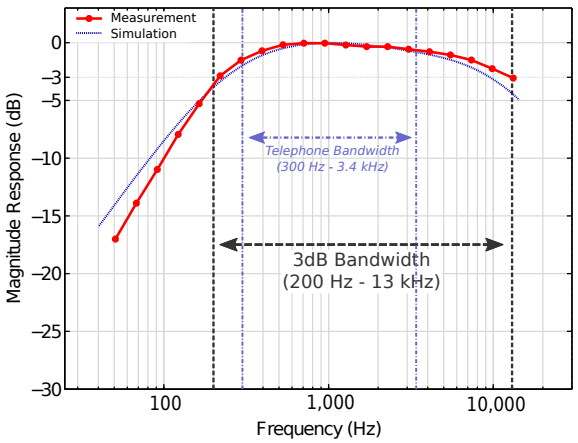

Fig. 3. Measured magnitude response of audio recording tag.

Additionally, we also present a modern, digital version of the Great Seal Bug, using the transponder's harvested DC voltage to passively power a built-in microphone. These demonstrations leverage a previously described platform originally designed for multichannel biotelemetry of neural and EMG signals in freely moving animals [13].

II. System Description

A block diagram of the system is shown in Fig. 1. The digital audio streaming system consists of two parts: the base station transceiver and the audio recording tag pictured in Fig. 2. The base station is responsible for RF carrier generation and transmission to the tag as well as data reception, demodulation and decoding. At the base station, a frequency synthesizer generates a frequency agile UHF (868–950 MHz) carrier that is passed through a power amplifier to yield a total output of +36 dBm EIRP, including transmit antenna gain. The base station is usually operated in a bistatic mode, with the signal captured by the receiving antenna of the base station being mixed with a replica of the transmitted carrier and passed through a set of analog bandpass filters and variable gain amplifier (VGA) blocks to shape the signal before being sent to an FPGA-based digital baseband processing unit. Analog baseband signals are sampled at 100 MS/s using a 16-bit analog to digital converter (ADC) and digitally filtered before being rotated and sliced for bit decisions, clock recovery and data decoding. The decoded data is sent to a PC over a USB connection for display and data capture.

The fully integrated audio transponder includes a 4-stage Schottky-diode based RF power harvester enabling fully-passive, battery-free operation, a 1.23 V low dropout (LDO) voltage regulator, a digitally-configurable, variable impedance backscatter binary phase shift keying (BPSK) modulator, digital logic for data encoding and packet framing, and 16 total amplifier channels including 10 audio bandwidth input channels each connected to an 11-bit ADC by a high-speed MUX. The IC itself requires a minimum of 3 off-chip components for operation – a miniature 20 MHz quartz crystal oscillator and two 0402 SMT bypass capacitors for the unregulated and regulated power supplies V_{DD} and $V_{DD-\mathrm{Reg}}$. The printed circuit board also includes an impedance matching network to transform the chip impedance to match the 50 Ω antenna impedance. The populated tag board, excluding an external antenna, measures 38 mm x 28 mm, with generous component spacing, so further reduction in size is straightforward.

The chip, developed at Intan Technologies, incorporates 10 fully differential low-noise, low-power CMOS front end amplifiers used for analog signal capture. The amplifiers have a simulated and measured bandwidth of 200 Hz – 13 kHz as shown in Fig. 3. For comparison, the bandwidth of the public switched telephone network (PSTN) is approximately 300–3400 Hz indicating that the tag has more than sufficient bandwidth available to faithfully reproduce human speech.

The on-chip amplifiers, originally designed for low-level neural signal recording, have a gain of $500\ V/V$ and a maximum input range of $\pm\ 2.4\ mV$. The chip uses an 11-bit ADC allowing the least significant bit (LSB) to represent $2.3\ \mu V$, referred to the input. Input-referred noise of the amplifier occupies 2-3 LSB's based on a measured input-referred noise value of $5.7\ \mu V_{\mathrm{rms}}$.

Each of the 10 input channels are sampled at a rate of 26.1 kS/s, connected one at a time to the ADC by a high-speed MUX. Additionally, the chip includes 4 lower bandwidth amplifier channels (originally designed for EMG signals) and 2 general purpose dc amplifiers which are also sampled by the ADC and transmitted. These auxiliary channels have not been characterized for audio throughput and are not currently utilized in this demonstration setup. The 11-bit sampled data from each of the 16 channels (10 audio channels + 6 unused channels) is encoded on-chip into a 16-bit word using an extended (11, 16) Hamming code providing robust data transmission by detecting double-bit errors and correcting single-bit errors. Each word, combined with a tag ID word, frame counter, and frame markers, forms a frame of 192 16-bit words transmitted at a rate of 1627.6 frames per second yielding a total throughput of 5 Mbps.

The binary data is transmitted using a variable impedance

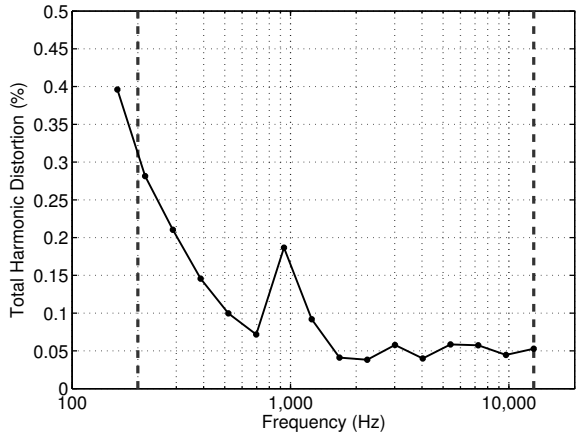

Fig. 4. Measured total harmonic distortion (THD + N).

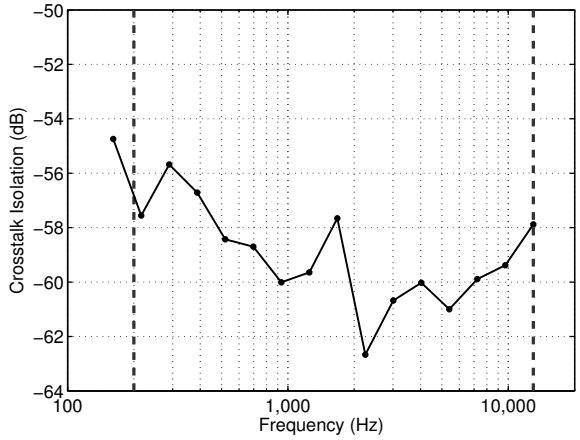

Fig. 5. Measured crosstalk between input amplifier channels.

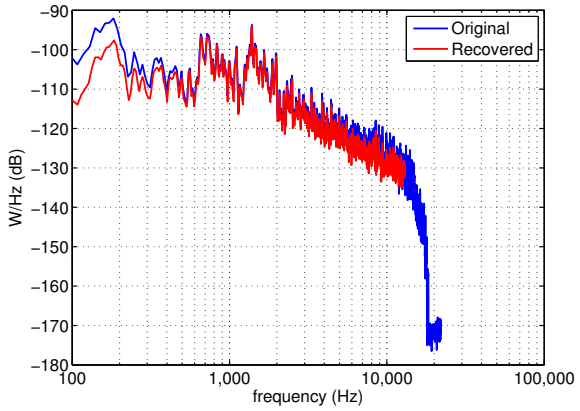

Fig. 6. Measured spectrum comparing original source audio signal and recovered audio signal (cabled setup).

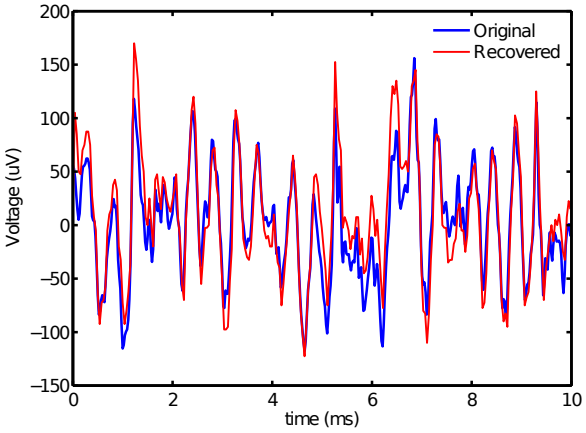

Fig. 7. Measured time-domain waveforms comparing original source audio signal and recovered audio signal (cabled setup).

binary phase shift keying (BPSK) modulator realized using a user-configurable, digitally selectable capacitor array connected in parallel with the antenna terminals through a single FET. Modulation depth is purposefully kept low to allow the majority of power to be absorbed by the RF harvesting circuit and varies between 0.22% – 1.74% $|\Delta\Gamma|$ referenced to the conjugate match impedance.

To understand their distortion performance in audio applications, the amplifier channels were characterized by measuring total harmonic distortion plus noise (THD + N) and channel crosstalk. The THD + N measurement was performed by injecting a single tone into the audio chip and recording the received signal. This test was performed in a cabled setup using a $50\ \Omega$ shielded cable and attenuators to approximate the over-the-air channel while maintaining minimum RF noise in the environment. The received data was filtered in post-processing with a digital notch filter (Q = 10) to remove the input tone, leaving only the resulting harmonics and noise for a single amplifier channel. THD was then calculated as the ratio of harmonic plus noise power to original signal power (including the fundamental tone)

$$\text{THD} + N = \frac{\sum \left(S_i^{\text{filt.}}\right)^2}{\sum \left(S_i\right)^2} \tag{1}$$

where $S_i^{\text{filt.}}$ is the filtered signal and S_i is the original signal including all harmonics. THD + N is then reported as a percentage. This measurement was taken over the entire signal bandwidth (dc – 13 kHz). Measured THD + N data, as shown in Fig. 4, is less than 0.3% over the entire 3 dB channel bandwidth.

Crosstalk between amplifier channels was also measured. Similar to the THD + N measurement, a single tone was injected into the input port of an amplifier channel (channel A) and the ratio of power levels between channel A and a terminated channel (channel B) was measured. The results shown in Fig. 5 show that isolation between channels remains better than -55 dB over the entire bandwidth (i.e. less than 0.00001% leakage between channels).

III. Digital Audio Characterization

Using a cabled channel setup, a stereo audio file containing music sampled at compact disk (CD) quality ($f_s = 44100$ Hz,

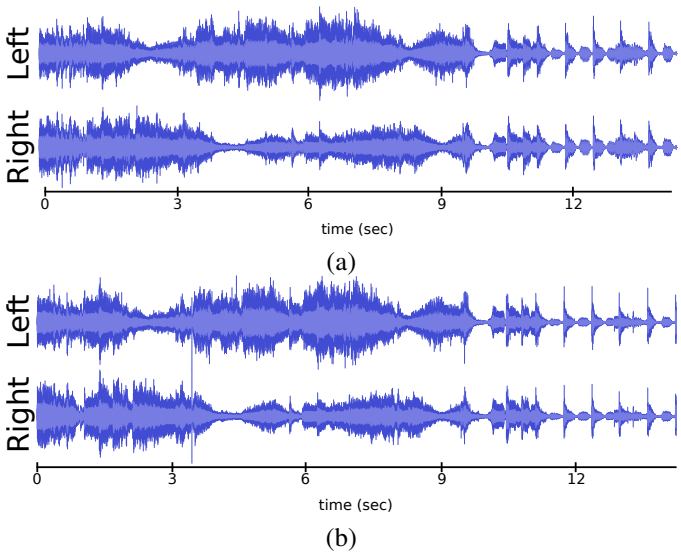

Fig. 8. Measured over-the-air recording comparing original, transmitted waveform (a) and received, recovered waveform (b).

16-bits) was played back, using a battery powered external device (Apple iPhone) as a signal source. The use of a battery powered audio source allows the testing to be independent of lab ground to avoid ground loops and/or unwanted 60 Hz hum pickup. After passing through the entire tag + RF channel + base station system, the received digital audio signal was then compared to the original recording. Based on an informal sampling of nearby listeners at the time of the experiment, listeners had difficulty differentiating between the original source and the received audio, even given the difference in sample depth and sample rate (16-bits vs. 11-bits, and 44.1 kHz vs. 26.1 kHz).

We then proceeded to perform a more formal engineering evaluation of signal fidelity. In Fig. 6 the frequency spectrum of the original, CD-quality recording is compared to the recovered audio transmitted through the audio transponder. Though some information is lost below ≈300 Hz and above 13 kHz (the Nyquist frequency of the on-chip ADC sampling rate), the overall shape of the spectrum is maintained. Similarity is also observed in the time-domain comparison, shown in Fig. 7. The recovered signal does not track the very highest-frequency features of the original signal, but follows the overall shape of the signal, still allowing for perceptually clear audio reproduction.

After confirmation of functionality of the audio transponder using the cabled setup, an over the air experiment was performed. In this experiment, the base station was configured to output +36 dBm EIRP, using a bistatic configuration with 8 dBi linear patch transmit and receive antennas. The audio transponder was attached to a similar 8 dBi linear patch antenna and placed 1.4 m away from the base station. A battery powered external device (Apple iPhone) was again used as the audio test source. The left and right stereo channels of the iPhone audio output were connected to two input channels of the tag and a CD-quality, stereo file was played back through the transponder and recorded at the base station.

TABLE I
WIRELESS POWER LINK BUDGET

Transmitter output power	P_t	+28 dBm
Transmitter antenna gain	G_t	8 dBi
Receiver (tag) antenna gain	G_r	8 dBi
Operating wavelength	λ	33 cm
Received power at tag input terminals	P_r	7.76 dBm
IC power harvester + mismatch efficiency	η	20.6 %
DC power consumed by tag	P_{th}	1.23 mW
Power-up threshold distance	$r\big\vert_{P_r = 7.76\,\text{dBm}}$	1.703 m

The original, stereo input signal played back into the audio transponder is shown in Fig. 8 (a) and again compared in the time domain to the received signal, recorded at the base station, shown in Fig. 8(b). Features of the music recording align correctly in time and amplitude and the stereo effects are also both visibly and audibly preserved. This over-the-air test demonstrates that it is possible to transfer high-quality, digitized audio recordings using backscatter technology at distances greater than 1 m. Though only two channels were connected to an audio source in this test, all 16 channels (10 available audio channels, 4 lower-bandwidth channels, and 2 general purpose dc channels) were simultaneously telemetered. Multiple channel pairs were tested with equivalent results; the lack of a 10-port audio test source prevented us from simultaneously testing all 10 channels but we are confident from pairwise testing that all channels are functioning equivalently.

A link budget is provided in Table I for the audio transponder. This table assumes a transmit power of +28 dBm, a transmit antenna with 8 dBi gain, operation at 915 MHz in freespace, and a tag antenna gain of 8 dBi. Based on a measured tag RF power-up threshold of 7.76 dBm, a maximum forward link limited operating distance of 1.703 m is predicted.

Using the calculation of receiver sensitivity presented in [13], for the measured receiver noise figure of 13 dB, input referred noise is -88 dBm. Assuming a 10 dB SNR yielding a bit error rate of approximately 10^{-5} for BPSK and an assumed backscatter ratio of 15 dB, a theoretical maximum operating distance of ≈14 m is predicted for the tag operating in semi-passive mode.

A. *Image Transfer via Modulated Backscatter*

The over-the-air setup described above was then used to transmit full-color images using slow-scan television modulation (SSTV) through the audio transponder. While the 5 Mbps uplink data rate provided by the tag could certainly be used to carry compressed digital video, we opted to leverage the existing audio-bandwidth pipeline for our initial experiments with image transfer via modulated backscatter.

SSTV is commonly employed by amateur radio enthusiasts for image transmission through narrowband radio channels as well as by NASA / NOAA polar orbiting weather satellites utilizing the Automatic Picture Transmission (APT) standard [14], [15]. In general, SSTV operates by converting an image to an analog audio-bandwidth signal by conveying pixel lumi-

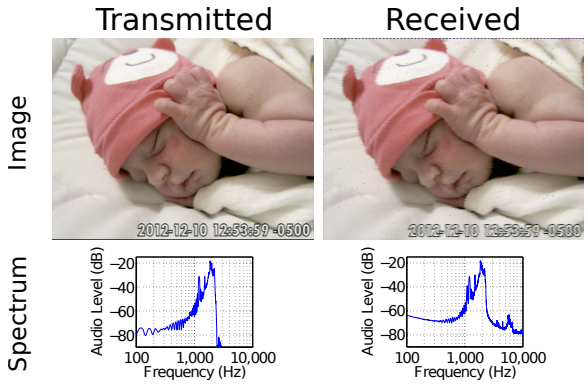

Fig. 9. Comparison of transmitted and received image using an SSTV modulation technique.

nance and color information via amplitude modulation (AM), frequency modulation (FM) or a combination of both. There exist many differing protocols for such types of transmission which have different frame rates and image quality parameters [16].

In this experiment, the *PD290* protocol was used to modulate a 640 x 493 pixel input image into an audio file. This protocol allows for transmission of full-color images, but requires long transmission times of 290 seconds per frame (≈5 min / frame). The software "Multi-Scan 2" for Macintosh OSX was used for encoding images into audio as well as decoding audio into images.

The input image, shown in Fig. 9 with audio spectrum, was chosen to represent a hypothetical application of a passive child-monitoring system. This encoded audio file was played back into the audio transponder using the Apple iPhone as a signal source and wirelessly telemetered 1.4 m to the base station. The received audio was captured and then decoded using the Multi-Scan 2 software. The recovered image and spectrum are shown in Fig. 9 on the right compared to the transmitted image on the left. Though some high-frequency noise is present in the received image, the subject is clearly visible and image fidelity is very good.

B. Battery-Free Digital Wireless Microphone

We then set out to update Theremin's analog Great Seal Bug with modern digital techniques. A very low power microphone (Knowles EM-23046-P16) was integrated with the audio transponder circuit. This microphone is specified for operation down to 1.3V VDD, with a current drain of 50μA maximum. Its frequency response is specified to include the region between 100 Hz and 5 kHz which is predominant in human speech.

The regulated 1.3V V_{reg} voltage output from the tag chip's RF voltage harvesting circuit was connected to the microphone. The analog voltage output from the microphone was passed through a voltage divider to reduce signal levels to those appropriate for the amplifier input. The circuit is shown in the block diagram of Fig. 1.

The audio transponder with its passive microphone was

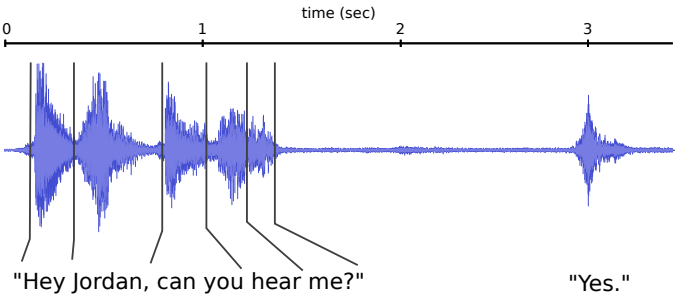

Fig. 10. Fully passive recording of a conversation between participants spaced approximately 3 m.

used in combination with a dipole tag antenna with estimated gain of approximately 4 dBi (wire dipole with quarter-wave reflector) and placed 0.72 m away from the base station configured to transmit +36 dBm. Based on a link budget similar to Table I but scaled for appropriate tag antenna gain, a theoretical maximum operating distance of 1.07 m is expected.

Fig. 10 presents a time-domain plot of a conversation recorded using the fully passive digital microphone.[1] The conversation presented is between two individuals located approximately 0.5 and 3 m respectively away from the microphone. In informal testing, the device recorded clearly audible conversation between participants located over 5 m from the microphone when speaking at normal conversation levels.

IV. Discussion and Conclusion

In this paper, we present the first wireless transfer of multichannel high-fidelity digital audio using a fully integrated, battery-free modulated backscatter transponder. We have also presented the transfer of stereo music, color still image transfer using SSTV (*PD290*), and an updated version of Theremin's Great Seal Bug providing fully passive digital recording of room sounds using a microphone powered by harvested voltage.

We believe these results will serve as a first step toward media-rich battery-free devices that take advantage of the high speed, low power nature of modulated backscatter communication links. Future work will focus on interfacing additional sensors on-tag, such as a CMOS camera sensor, in addition to the microphone. The achieved backscatter data link rate of 5 Mbps is more than sufficient for multichannel digital audio and compressed motion video. We expect that ongoing research in power-efficient audio and video codec hardware and software already being developed for smartphone applications will enable increasing media-rich functions even on highly power constrained devices with μW to mW power budgets. This work demonstrates the potential of a new class of media-rich, battery-free devices with unlimited lifetime and great operational flexibility.

[1]The data shown in Fig. 10 was filtered in post-processing to remove room noise before plotting, using the "Noise Removal" tool from the open-source software Audacity. This tool removed high frequency room noise to show the conversation more clearly in the figure, though even with no filtering applied, recorded conversation is easily distinguishable in the raw recordings.

ACKNOWLEDGMENT

This work was supported in part by the Howard Hughes Medical Institute. The authors would like to thank fellow lab participants Jordan Besnoff, Joshua Ensworth, and Daniel Arnitz for volunteering to listen and compare audio files, be it willingly or not.

REFERENCES

[1] A. G. Bell, "Upon the production and reproduction of sound by light," *Journal of the Society of Telegraph Engineers*, vol. 9, no. 34, pp. 404–426, 1880.

[2] P. Nikitin, "Leon Theremin (Lev Termen)," *IEEE Antennas and Propagation Magazine*, vol. 54, no. 5, pp. 252 – 257, October 2012.

[3] H. Stockman, "Communication by means of reflected power," *Proceedings of the IRE*, vol. 36, no. 10, pp. 1196–1204, October 1948.

[4] A. Koelle, S. Depp, and R. Freyman, "Short-range radio-telemetry for electronic identification, using modulated RF backscatter," *Proceedings of the IEEE*, vol. 63, no. 8, pp. 1260 – 1261, August 1975.

[5] U. Karthaus and M. Fischer, "Fully integrated passive UHF RFID transponder IC with 16.7-μW minimum RF input power," *IEEE Journal of Solid-State Circuits*, vol. 38, no. 10, pp. 1602–1608, October 2003.

[6] R. Want, "Enabling ubiquitous sensing with RFID," *Computer*, vol. 37, no. 4, pp. 84–86, April 2004.

[7] A. Sample, D. Yeager, P. Powledge, A. Mamishev, and J. Smith, "Design of an RFID-based battery-free programmable sensing platform," *IEEE Transactions on Instrumentation and Measurement*, vol. 57, no. 11, pp. 2608–2615, November 2008.

[8] D. Yeager, F. Zhang, A. Zarrasvand, N. George, R. Daniel, and B. Otis, "A 9μA, addressable Gen2 sensor tag for biosignal acquisition," *IEEE Journal of Solid-State Circuits*, vol. 45, no. 10, pp. 2198–2209, Oct. 2010.

[9] EPC Global US, "Class 1 Generation 2 UHF RFID protocol for operation at 860MHz-960MHz, version 1.0.9," Available online, *http://www.epcglobalus.org/*, 2005.

[10] Y. Maguire and R. Pappu, "An optimal Q-algorithm for the ISO 18000-6C RFID protocol," *IEEE Transactions on Automation Science and Engineering*, vol. 6, no. 1, pp. 16–24, January 2009.

[11] Thomas, S. J. and Wheeler, E. and Teizer, J. and Reynolds, M. S., "Quadrature Amplitude Modulated Backscatter in Passive and Semipassive UHF RFID Systems," *IEEE Transactions on Microwave Theory and Techniques*, vol. 60, no. 4, pp. 1175–1182, April 2012.

[12] Thomas, S. J. and Reynolds, M. S., "A 96 Mbit/sec, 15.5 pJ/bit 16-QAM Modulator for UHF Backscatter Communication," in *2012 IEEE International Conference on RFID*, April 2012, pp. 185–190.

[13] Thomas, S. J. and Harrison, Reid R. and Leonardo, Anthony and Reynolds, M. S., "A battery-free multi-channel digital neural/EMG telemetry system for flying insects," *IEEE Transactions on Biomedical Circuits and Systems*, vol. 6, no. 5, pp. 424–436, October 2012.

[14] R. Stampfl, "The NIMBUS spacecraft and its communication system as of September 1961," *NASA Technical Note D-1422*, 1963.

[15] NOAA Satellite and Information Service, "Polar operational environmental satellite," 2013, [Online; accessed 4-January-2013]. [Online]. Available: http://www.oso.noaa.gov/poes/

[16] M. Bruchanov, "Image communication on short waves," September 2012, [Online; accessed 4-January-2013]. [Online]. Available: http://www.sstv-handbook.com